

ON PULSATILE HYDROMAGNETIC FLOW OF AN OLDROYD FLUID  
WITH HEAT TRANSFER

S. S r i n i v a s<sup>1)</sup>, T. M a l a t h y<sup>1)</sup>, P. L. S a c h d e v<sup>2)</sup>

<sup>1)</sup>Department of Mathematics  
Vellore Institute of Technology  
Deemed University  
Vellore – 632 014, India

<sup>2)</sup> Department of Mathematics  
Indian Institute of Science  
Bangalore

The problem of heat transfer to pulsatile flow of hydromagnetic viscoelastic fluid has been studied. Expressions for the velocity, temperature distribution and mass flow rate are obtained. The rate of heat transfer at the plates has also been calculated. These expressions are evaluated numerically for various values of the parameters. The influence of pertinent parameters on temperature, heat transfer coefficient and mass flux has been studied and numerical results obtained are presented graphically.

**Key words:** Pulsatile flow, Oldroyd fluid, Hartmann number and heat transfer.

1. INTRODUCTION

The problems of fluid flow in a channel or pipe have been studied in recent past by many scientists [1–7] with a focus to understand some physical phenomena such as transpiration cooling and gaseous diffusion. In recent years, considerable attention has been given to problems of heat transfer to pulsatile fluid flows [7, 9–16]. The solutions of these problems play a vital role in the study of blood flow in arteries [8, 17]. RADHAKRISHNAMACHARYA and MAITI [9] have made an investigation of heat transfer to pulsatile viscous fluid flow in a porous channel. Later GHOSH and DEBNATH [11] analyzed the problem of heat transfer to pulsatile flow in a viscoelastic fluid bounded by impervious rigid parallel plates.

The present paper considers the heat transfer to the pulsatile hydromagnetic flow of a viscoelastic fluid bounded by impervious rigid parallel plates separated by a distance  $h$ . The fluid is driven by an unsteady pressure gradient. With the assumption that the upper plate is at a temperature higher than the lower one, the solutions for the steady and fluctuating temperature distributions are

obtained. The rate of heat transfer at the plates is also calculated. Numerical solutions are discussed with graphical representations. It is found that elastic properties of the fluid significantly increase the temperature in the boundary layers near the plates. The magnitude of heat transfer at the plates is also greatly affected by elasticity of the fluid and the Eckert number.

## 2. MATHEMATICAL FORMULATION

We consider the pulsatile flow of a viscoelastic fluid between two infinitely long parallel plates, at a distance  $h$  apart, which is driven by the unsteady pressure gradient

$$(2.1) \quad -\frac{1}{\rho} \frac{\partial p}{\partial x} = A \{1 + \varepsilon \exp(i\omega t)\},$$

where  $A$  is a known constant,  $\varepsilon$  is a suitably chosen positive quantity and  $\omega$  is the frequency. Let the  $x$ -axis be along one plate and  $y$ -axis normal to it. The plate  $y = 0$  and  $y = h$  are maintained at uniform temperatures  $T_0$  and  $T_1 (> T_0)$  respectively. It is assumed that the motion is slow so that all second-order quantities may be neglected. A uniform magnetic field is imposed along the direction normal to the flow. In the analysis, we assume that the induced magnetic field is negligible.

This study is based upon the Oldroyd model of a viscoelastic fluid [6], and the properties of such a fluid are specified by three constants  $\eta_0$ , of the dimension of viscosity, and  $\lambda_1, \lambda_2$  of dimensions of time. The equations of the state relating to stress tensor  $p_{ik}$  and the rate of strain tensor  $e_{ik} = \frac{1}{2}(u_{i,k} + u_{k,i})$  of such fluids are of the form

$$(2.2) \quad p_{ik} = p'_{ik} - p\delta_{ik},$$

$$(2.3) \quad \left(1 + \lambda_1 \frac{\partial}{\partial t}\right) p'_{ik} = 2\eta_0 \left(1 + \lambda_2 \frac{\partial}{\partial t}\right) e_{ik},$$

where  $u_i$  denotes the velocity vector,  $\delta_{ik}$  is the Kronecker delta,  $p_{ik}$  is the part of the stress tensor related to the change of the shape of a material element, and  $p$  is an isotropic pressure. The liquid ( $e_{ii} = 0$ ) described by the above model behaves as a viscous liquid if  $\eta_0 > 0$  and  $\lambda_1 = \lambda_2$ . The equations of motion combined with constitutive equations of the hydromagnetic viscoelastic fluid are given by

$$(2.4) \quad \left(1 + \lambda_1 \frac{\partial}{\partial t}\right) \frac{\partial u}{\partial t} = -\frac{1}{\rho} \left(1 + \lambda_1 \frac{\partial}{\partial t}\right) \frac{\partial p}{\partial x} + \nu \left(1 + \lambda_2 \frac{\partial}{\partial t}\right) \frac{\partial^2 u}{\partial y^2} - \left(1 + \lambda_1 \frac{\partial}{\partial t}\right) \frac{\sigma B_0^2 u}{\rho},$$

$$(2.5) \quad 0 = -\frac{1}{\rho} \left( 1 + \lambda_1 \frac{\partial}{\partial t} \right) \frac{\partial p}{\partial y},$$

where  $u$  is the fluid velocity in the  $x$ -direction,  $\sigma$  is the electrical conductivity and  $B_0$  is an imposed uniform magnetic field. The energy equation is

$$(2.6) \quad \rho C_p \frac{\partial T}{\partial t} = \chi \frac{\partial^2 T}{\partial y^2} + \mu \left( \frac{\partial u}{\partial y} \right)^2,$$

where  $\rho, C_p, \chi, \mu, \nu$  are respectively the density, specific heat, thermal conductivity, coefficient of dynamic viscosity and coefficient of kinematic viscosity, and  $\lambda_1$  and  $\lambda_2$  are the relaxation and retardation times respectively.

The boundary conditions are

$$(2.7) \quad u = 0, \quad T = T_0 \quad \text{at} \quad y = 0,$$

$$(2.8) \quad u = 0, \quad T = T_1 \quad \text{at} \quad y = h.$$

The solution of (2.4) has the form

$$(2.9) \quad u^* = \frac{u}{\left( \frac{Ah^2}{\nu} \right)} = u_0 + \varepsilon u_1 e^{i\tau}; \quad \tau = \omega t,$$

where

$$(2.10) \quad u_0 = \frac{1}{H^2} \left\{ 1 - \frac{\sinh H(1-\eta) + \sinh H\eta}{\sinh H} \right\},$$

$$(2.11) \quad u_1 = \frac{1}{\beta_2^2} \left\{ 1 - \frac{\sinh \beta_1(1-\eta) + \sinh \beta_1\eta}{\sinh \beta_1} \right\}$$

with

$$\eta = \frac{y}{h}, \quad H^2 = \frac{h^2 \sigma B_0^2}{\mu}, \quad R_*^2 = \frac{\omega h^2}{\nu}, \quad \nu = \frac{\mu}{\rho}, \quad \beta^2 = \frac{1 + iF_1}{1 + iF_1 F_2},$$

$$(2.12) \quad F_1 = \lambda_1 \omega, \quad F_2 = \frac{\lambda_2}{\lambda_1} (< 1),$$

$$\beta_1^2 = \beta^2 (H^2 + iR_*^2), \quad \beta_2^2 = H^2 + iR_*^2$$

It can be noted that the results for viscous fluid correspond to the case  $\lambda_2 = \lambda_1$ , i.e.  $F_2 = 1$ , independent of the values of  $F_1$ .

Introducing (2.12) and the dimensionless temperature

$$(2.13) \quad \theta = \frac{T - T_0}{T_1 - T_0}$$

in (2.6), the energy equation becomes

$$(2.14) \quad R_*^2 \frac{\partial \theta}{\partial \tau} = \frac{1}{P_r} \left( \frac{\partial^2 \theta}{\partial \eta^2} \right) + E_c \left( \frac{\partial u^*}{\partial \eta} \right)^2,$$

where  $P_r = \frac{\mu C_p}{\chi}$  is the Prandtl number, and  $E_c = \frac{A^2 h^4}{\nu^2 C_p (T_1 - T_0)}$  is the Eckert number. The boundary conditions for  $\theta$  are

$$(2.15) \quad \theta = 0 \quad \text{at} \quad \eta = 0,$$

$$(2.16) \quad \theta = 1 \quad \text{at} \quad \eta = 1.$$

In view of (2.9), the temperature  $\theta$  can be assumed in the form

$$(2.17) \quad \theta(\eta, t) = \theta_0(\eta) + \varepsilon F(\eta) e^{i\tau} + \varepsilon^2 G_1(\eta) e^{2i\tau}.$$

Substituting (2.17) and  $u^*$  in (2.14), equating the harmonic terms, retaining coefficients of  $\varepsilon^2$  and solving the corresponding equations for  $\theta_0, F(\eta)$  and  $G_1(\eta)$  with the help of (2.15) and (2.16), we obtain

$$(2.18) \quad \theta_0(\eta) = \eta + \frac{P_r E_c}{4H^2} \left\{ \eta(\eta - 1) \left[ 1 - \frac{(\cosh H - 1)^2}{\sinh^2 H} \right] + 2 \left[ \frac{\cosh H - 1}{H^2 \sinh^2 H} \right] \sinh H \eta \cdot \sinh H (1 - \eta) \right\},$$

$$(2.19) \quad F(\eta) = -L(0) \left\{ \cosh N \eta + \left( \frac{1 - \cosh N}{\sinh N} \right) \sinh N \eta \right\} + L(\eta),$$

$$(2.20) \quad L(\eta) = -\frac{4\beta_1 P_r E_c}{\beta_1^2 H \sinh H \cdot \sinh \beta_1} \cdot \sinh \left( \frac{H}{2} \right) \sinh \left( \frac{\beta_1}{2} \right) \left\{ \frac{1}{\beta_1^2 - N^2 + H(H + 2\beta_1)} \cosh \left[ \frac{(H + \beta_1)(1 - 2\eta)}{2} \right] - \frac{1}{\beta_1^2 - N^2 + H(H - 2\beta_1)} \cosh \left[ \frac{(H - \beta_1)(1 - 2\eta)}{2} \right] \right\},$$

$$(2.21) \quad L(0) = L(1) = -\frac{4\beta_1 P_r E_c}{\beta_2^2 H \sinh H \cdot \sinh \beta_1} \cdot \sinh\left(\frac{H}{2}\right) \sinh\left(\frac{\beta_1}{2}\right) \\ \left\{ \frac{1}{\beta_1^2 - N^2 + H(H + 2\beta_1)} \cosh\left(\frac{H + \beta_1}{2}\right) \right. \\ \left. - \frac{1}{\beta_1^2 - N^2 + H(H - 2\beta_1)} \cosh\left(\frac{H - \beta_1}{2}\right) \right\},$$

where

$$(2.22) \quad N = n(1 + i), \quad n = R_* \left(\frac{P_r}{2}\right)^{1/2},$$

and

$$(2.23) \quad G_1(\eta) = -\frac{1}{\sinh \sqrt{2}N} \left[ G_2(0) \sinh \sqrt{2}N(1 - \eta) \right. \\ \left. + G_2(1) \sinh \sqrt{2}N\eta \right] + G_2(\eta),$$

$$(2.24) \quad G_2(\eta) = \frac{P_r E_c \beta_1^2}{2\beta_2^4 \sinh^2 \beta_1} \left[ \frac{1 - \cosh \beta_1}{N^2} \right. \\ \left. - \left( \frac{1 + \cosh 2\beta_1 - 2 \cosh \beta_1}{2(2\beta_1^2 - N^2)} \right) \cosh 2\beta_1 \eta \right. \\ \left. + \frac{(\sinh 2\beta_1 - 2 \sinh \beta_1)}{2(2\beta_1^2 - N^2)} \sinh 2\beta_1 \eta \right],$$

$$(2.25) \quad G_2(0) = G_2(1) = \frac{P_r E_c \beta_1^2}{2\beta_2^4 \sinh^2 \beta_1} \left[ \frac{1 - \cosh \beta_1}{N^2} \right. \\ \left. - \left( \frac{1 + \cosh 2\beta_1 - 2 \cosh \beta_1}{2(2\beta_1^2 - N^2)} \right) \right].$$

The instantaneous mass flux  $Q$  may be obtained by integrating Eq. (2.9) across the channel:

$$(2.26) \quad \frac{Q}{\left(\frac{Ah^3}{\nu}\right)} = \frac{1}{H^2} \left[ 1 + 2 \left( \frac{1 - \cosh H}{H \sinh H} \right) \right] + \frac{\varepsilon^{i\omega t}}{\beta_2^2} \left[ 1 + 2 \left( \frac{1 - \cosh \beta_1}{\beta_1 \sinh \beta_1} \right) \right].$$

## 3. RATE OF HEAT TRANSFER

The rate of heat transfer per unit area at the plate  $\eta = 0$  is given by

$$\begin{aligned}
Q'_0 &= -\frac{q_0 h}{\chi(T_1 - T_0)} = \left( \frac{\partial \theta}{\partial \eta} \right)_{\eta=0}, \\
Q'_0 &= \left( \frac{d\theta_0}{d\eta} \right)_{\eta=0} + \varepsilon e^{i\omega t} \left( \frac{dF}{d\eta} \right)_{\eta=0} + \varepsilon^2 e^{2i\omega t} \left( \frac{dG_1}{d\eta} \right)_{\eta=0}, \\
(3.1) \quad Q'_0 &= 1 + \frac{Pr Ec}{H^2} \left\{ \left( \frac{\cosh H - 1}{\sinh^2 H} \right) \left( \frac{2 \sinh H}{H} + (\cosh H - 1) \right) - 1 \right\} \\
&+ \varepsilon e^{i\omega t} \left[ \frac{-NL(0)}{\sinh N} (1 - \cosh N) + \frac{4\beta_1 Pr Ec}{\beta_2^2 H \sinh H \sinh \beta_1} \cdot \sinh \left( \frac{H}{2} \right) \sinh \left( \frac{\beta_1}{2} \right) \right. \\
&\left. \left\{ \frac{(H + \beta_1) \sinh \left( \frac{H + \beta_1}{2} \right)}{\beta_1^2 - N^2 + H(H + 2\beta_1)} - \frac{(H - \beta_1) \sinh \left( \frac{H - \beta_1}{2} \right)}{\beta_1^2 - N^2 + H(H - 2\beta_1)} \right\} + \varepsilon^2 e^{2i\omega t} \right. \\
&\left. \left\{ \frac{-G_2(0) \sqrt{2} N}{\sinh \sqrt{2} N} (1 + \cosh \sqrt{2} N) + \frac{Pr Ec \beta_1^3 (\sinh 2\beta_1 - 2 \sinh \beta_1)}{2\beta_2^4 (2\beta_1^2 - N^2) \sinh^2 \beta_1} \right\} \right] \\
&= (\theta'_0)_{\eta=0} + \varepsilon |D_0| \cos(\omega t + \alpha_0) + \dots,
\end{aligned}$$

where  $D_0 = D_{0r} + iD_{0i}$  and  $\tan \alpha_0 = D_{0i}/D_{0r}$ .

Similarly, the rate of heat transfer per unit area at the plate  $\eta = 1$  is given by

$$\begin{aligned}
Q'_1 &= -\frac{q_1 h}{\chi(T_1 - T_0)} = \left( \frac{\partial \theta}{\partial \eta} \right)_{\eta=1}, \\
(3.2) \quad Q'_1 &= 1 + \frac{Pr Ec}{H^2} \left[ 1 - \left( \frac{\cosh H - 1}{\sinh^2 H} \right) \left( (\cosh H - 1) + \frac{2 \sinh H}{H} \right) \right] \\
&+ \varepsilon e^{i\omega t} \left\{ -NL(0) \left( \sinh N + \left( \frac{1 - \cosh N}{\sinh N} \right) \cosh N \right) \right\}
\end{aligned}$$

$$\begin{aligned}
(3.2) \quad & - \frac{4\beta_1 P_r E_c}{\beta_2^2 H \sinh H \sinh \beta_1} \cdot \sinh\left(\frac{H}{2}\right) \sinh\left(\frac{\beta_1}{2}\right) \\
\text{[cont.]} \quad & \left[ \frac{H + \beta_1}{\beta_1^2 - N^2 + H(H + 2\beta_1)} \cdot \sinh\left(\frac{H + \beta_1}{2}\right) \right. \\
& \left. - \frac{(H - \beta_1)}{\beta_1^2 - N^2 + H(H - 2\beta_1)} \sinh\left(\frac{H - \beta_1}{2}\right) \right] \Bigg\} \\
& + \varepsilon^2 e^{2i\omega t} \left\{ \frac{-\sqrt{2} N G_2(0)}{\sinh \sqrt{2} N} [\cosh \sqrt{2} N - 1] + \frac{P_r E_c \beta_1^3}{\beta_2^4 \sinh^2 \beta_1} \right. \\
& \left. \left[ \left( \frac{\sinh 2\beta_1 - 2 \sinh \beta_1}{2(2\beta_1^2 - N^2)} \right) \cosh 2\beta_1 - \left( \frac{1 + \cosh 2\beta_1 - 2 \cosh \beta_1}{2(2\beta_1^2 - N^2)} \right) \sinh 2\beta_1 \right] \right\} \\
& = (\theta'_0)_{\eta=1} + \varepsilon |D_1| \cos(\omega t + \alpha_1) + \dots,
\end{aligned}$$

where  $D_1 = D_{1r} + iD_{1i}$  and  $\tan \alpha_1 = D_{1i}/D_{1r}$ .

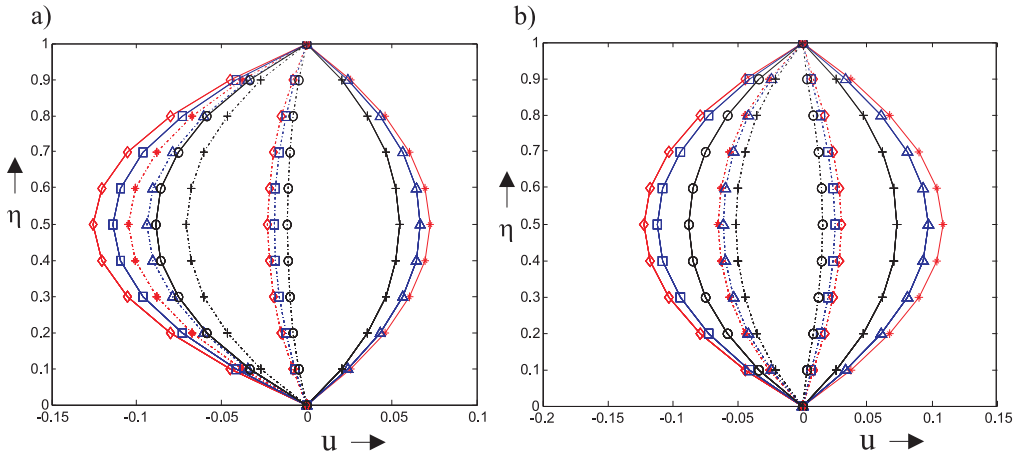
#### 4. NUMERICAL RESULTS AND DISCUSSION

In order to get the physical insight of the problem, velocity, temperature field, mass flow and rate of heat transfer have been discussed by assigning numerical values to various parameters obtained in mathematical formulation of the problem and the results are shown graphically.

From Fig. 1a, it can be observed that when the frequency  $R_*$  is small, the unsteady velocity profile is almost parabolic. Also it can be noted that the unsteady velocity decreases with the increasing values of the Hartmann number. Part of the unsteady velocity profile is nearly linear as the frequency increases and the maximum occurs in the central part of the channel, Fig. 1b. If the frequency is large, the maxima of the velocity are shifted to the boundary layers near the walls, Figs. 1c and 1d.

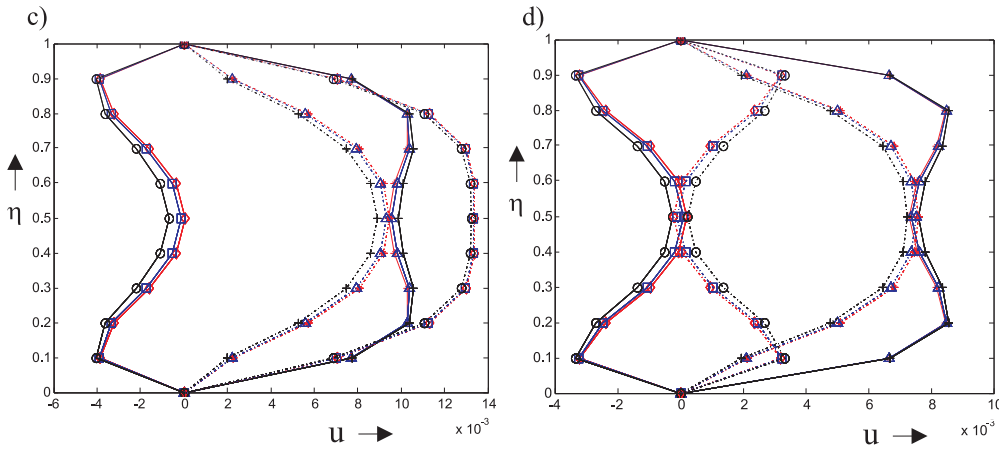
The effects of the velocity profiles for different values of the Hartmann number and frequency parameter are shown in Figs. 2a and 2b. It can be observed from Fig. 2a that the velocity  $u$  of the fluid in the  $x$ -direction decreases due to increase of the Hartmann number  $H$ . As the frequency parameter increases, we can note from Figs. 2b and 2c that velocity decreases

The magnitude of the mass flux of  $\frac{Q\nu}{Ah^3}$  is plotted in Figs. 3a and 3b. It can be observed that mass flux decreases as the frequency parameter and Hartmann number increases.



$$F_1 = 0.2, F_2 = 0.08, P_r = 100, R_* = 0$$

$$F_1 = 0.2, F_2 = 0.08, P_r = 100, R_* = 2$$



$$F_1 = 0.2, F_2 = 1, P_r = 100, R_* = 9$$

$$F_1 = 0.2, F_2 = 1, P_r = 100, R_* = 10$$

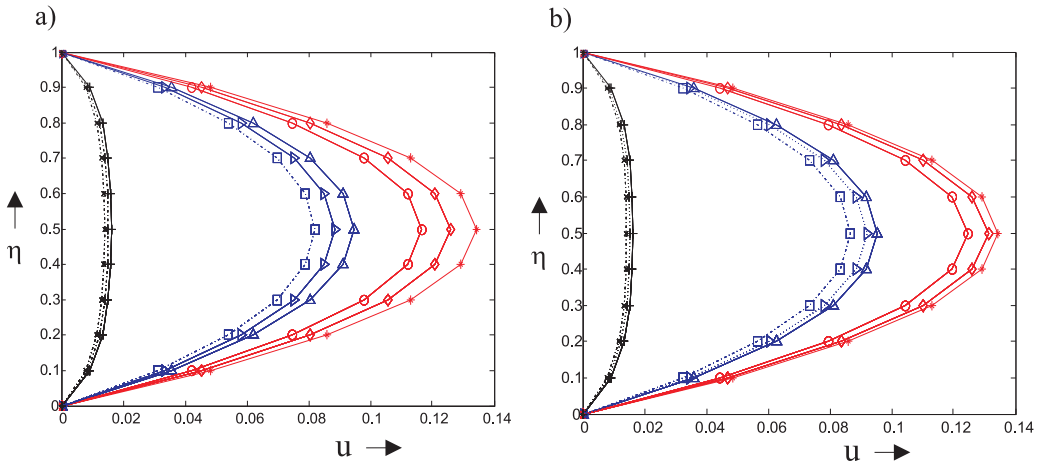
$$* \text{---} * \quad H = 0, \quad \Delta \text{---} \Delta \quad H = 1, \quad + \text{---} + \quad H = 2, \quad \omega t = \pi/4$$

$$\diamond \text{---} \diamond \quad H = 0, \quad \square \text{---} \square \quad H = 1, \quad o \text{---} o \quad H = 2, \quad \omega t = \pi/2$$

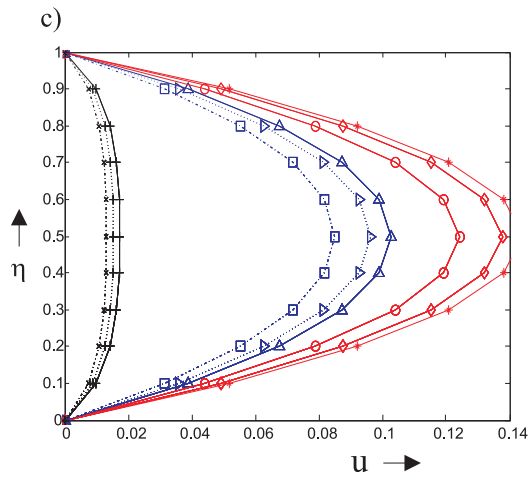
$$* \text{---} * \quad H = 0, \quad \Delta \text{---} \Delta \quad H = 1, \quad + \text{---} + \quad H = 2, \quad \omega t = 3\pi/4$$

$$\diamond \text{---} \diamond \quad H = 0, \quad \square \text{---} \square \quad H = 1, \quad o \text{---} o \quad H = 2, \quad \omega t = \pi$$

FIG. 1. Unsteady velocity profiles.



$F_1 = 0.2, F_2 = 0.8, P_r = 100, R_* = 1, \varepsilon = 0.1$      $F_1 = 0.2, F_2 = 0.8, P_r = 100, R_* = 3, \varepsilon = 0.1$



$F_1 = 0.2, F_2 = 0.8, P_r = 100, R_* = 3, \varepsilon = 0.2$

*—*	$H = 0,$	$\Delta$ — $\Delta$	$H = 2,$	+—+	$H = 8,$	$\omega t = \pi/4$
$\diamond$ — $\diamond$	$H = 0,$	$\triangleright$ — $\triangleright$	$H = 2,$	+—·—+	$H = 8,$	$\omega t = \pi/2$
o—o	$H = 0,$	$\square$ —·— $\square$	$H = 2,$	$\times$ —·— $\times$	$H = 8,$	$\omega t = 3\pi/4$

FIG. 2. Velocity profiles.

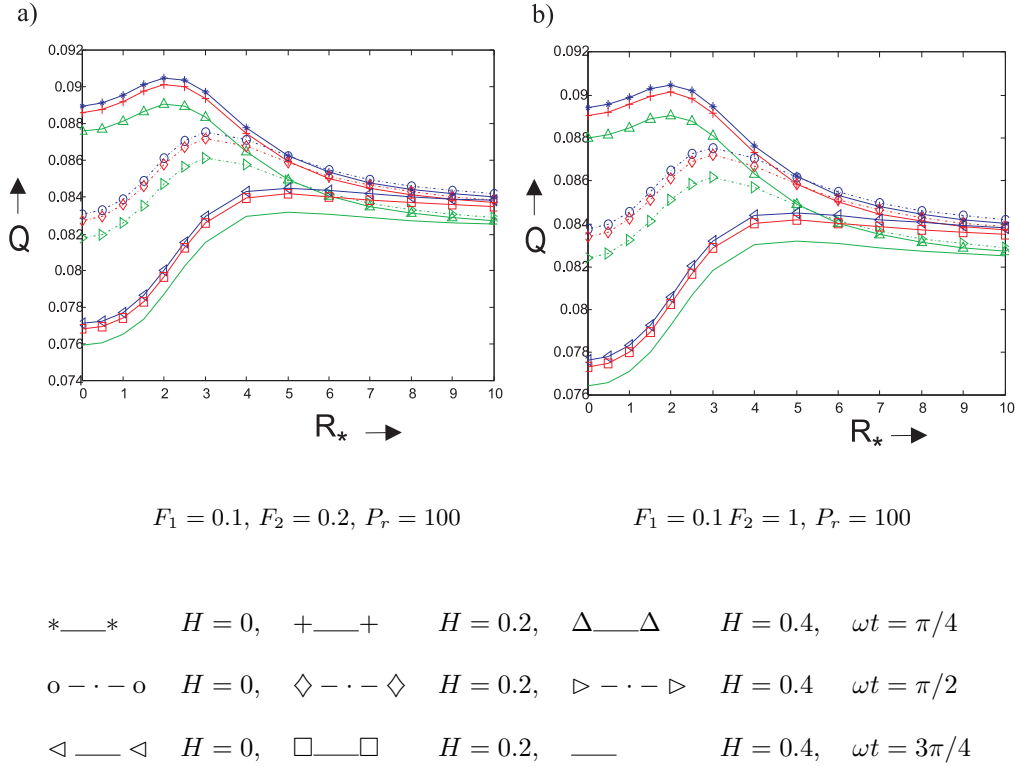
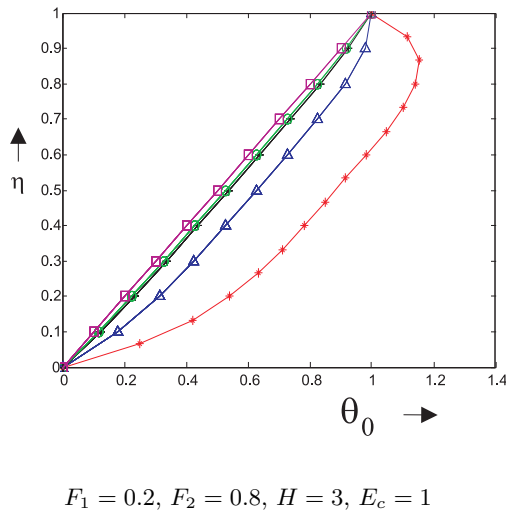
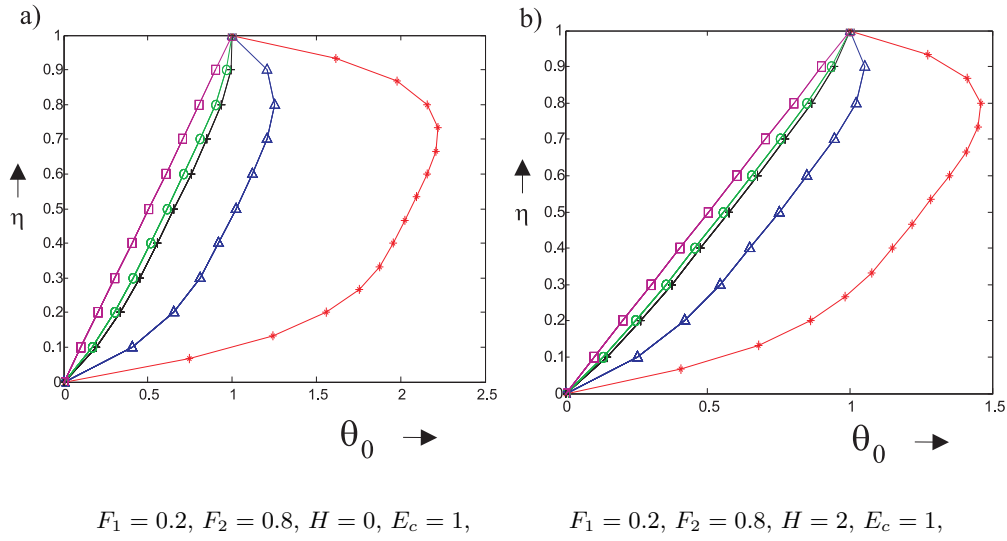


FIG. 3. Magnitude of the mass flux.

In the problem under investigation,  $\theta_0$  represents the steady temperature distribution in the fluid. The expression for  $\theta_0$  given by (2.18) remains the same for both a viscous and a viscoelastic fluid of Oldroyd type under similar conditions. Figure 4 depicts the steady temperature profiles corresponding to  $\theta_0$  for various values of  $P_r E_c$ . The steady temperature profiles plotted in Figs. 4a, 4b, 4c are almost parabolic and temperature decreases with increase of the Hartmann number. Further it can be noticed that the increase in Hartmann number decreases the rate of heat transfer. We note that there is no change in the character of the profiles as  $E_c$  varies. But as the Eckert number  $E_c$  increases, the steady temperature increases. Regarding the rate of heat transfer in the steady – state condition the reversal of heat flux from the fluid to the hotter plate takes place when  $P_r E_c > 22$  which, in turn, makes the hotter plate more hot. In fact, the value of  $P_r E_c$  provides a measure of the amount of heat generated due to friction which, in the present case, increases with the increase of the pressure gradient. If the temperature difference between the plates is fixed, heat flows



\*—\*  $P_r = 300,$      $\Delta$ — $\Delta$   $P_r = 100,$     +—+  $P_r = 30,$   
 o—o  $P_r = 22,$      $\square$ — $\square$   $P_r = 1.$

FIG. 4. Steady temperature profiles.

from the hotter plate to the fluid as long as the pressure gradient does not exceed a certain value, i.e for  $P_r E_c$  to be not greater than 22. This phenomenon

is important for cooling at high pressure gradients. The effect of changing the Hartmann number (for fixed  $E_c$ ) and changing Eckert number (for fixed  $H$ ) are shown in Tables 1 and 2. Table 1 shows that the rate of heat transfer from the lower plate decreases with Hartmann number, whereas it increases in the upper plate. We observe from Table 2 that the rate of heat transfer from the lower plate increases with  $E_c$  while at the upper plate, the heat flows from the fluid to the plate even if  $T_1 > T_0$ .

**Table 1.**

$$E_c = 1, P_r = 100, R_* = 1$$

	$H = 0$	$H = 1$	$H = 2$	$H = 3$
$(\theta'_0)_{\eta=0}$	17.6518	14.7787	9.5485	5.69695
$(\theta'_0)_{\eta=1}$	-15.6518	-12.7787	-7.5405	-3.6969

**Table 2.**

$$P_r = 10, H = 1.5, R_* = 1$$

	$E_c = 1$	2	3	5
$(\theta'_0)_{\eta=0}$	2.1123	3.2247	4.3371	6.5618
$(\theta'_0)_{\eta=1}$	-0.11235	-1.22471	-2.33706	-4.56177

Fixing  $P_r$  and  $R_*$ , the instantaneous temperature profiles are plotted in Figs. 5a–5e, enabling us to observe the effect of changing  $H$  (with  $E_c$  fixed) and changing  $E_c$  (with  $H$  fixed). It also depicts the effect of changing values of the elastic parameters  $F_1$  and  $F_2$ . It can be noted that  $F_2 = 1$  always represent the case of a viscous fluid irrespective of the values of  $F_1$ . From Figs. 5a–5e, it can be seen that temperature decreases as  $H$  increases. The temperature profiles are almost parabolic for small values of  $H$ , but they oscillate more for large values of  $H$  and the maximum temperature is shifted to the boundary layers near the walls. The temperature increases rapidly with increase in  $E_c$ , which may be due to high viscous dissipation. Comparison of Figs. 5b and Fig. 5c shows that the presence of the elasticity of the fluid increases the temperature in a region near the plate and gradually diminishes the same at the central part of the channel. This study indicates that the temperature in a viscoelastic fluid increases rapidly with the increase of  $E_c$  and also interestingly we find that the increase of temperature near the plate occurs mainly due to the increase of the relaxation time of the fluid, while the increase in retardation time of the fluid produces a gradual decrease of temperature at the central part of the channel. It can be

observed that there is no significant change in the character of the profile as  $E_c$  varies.

The effect of changing elastic parameters and changing  $H$  (for fixed  $E_c$ ) and changing  $R_*$  (for fixed  $E_c$ ) and changing  $E_c$  (for fixed  $H$ ), on the values of the amplitude and phase of the rate of heat transfer is shown in Tables 3, 4 and 5. In Table 3, it is observed for a viscoelastic fluid the increase in Hartmann number decreases the amplitude of heat transfer at both the plates. There is a phase lag at both the plates when the fluid is viscoelastic. It may be observed from Table 4 that at the lower plate there is a phase lag at higher frequency, but at the upper plate there is a phase lead. We also find that at both the plates the amplitude decreases uniformly with frequency for fixed  $E_c$ . It can be noticed from Table 5 for fixed  $R_*$  the amplitude increases uniformly with  $E_c$  at both the walls. The increase of the Eckert number  $E_c$  increases the amplitude of heat transfer at the plates for the viscoelastic fluid, while the phase at the plates remains unaffected by the increase of  $E_c$ .

**Table 3.**

$$P_r = 200, R_* = 10, F_1 = 0.1, F_2 = 0.5, E_c = 3$$

$H$	$ D_0 $	$ D_1 $	$\tan \alpha_0$	$\tan \alpha_1$
0	0.261855	0.0231703	-29.0306	12.9313
0.2	0.260977	0.0231044	-28.8304	12.8729
0.4	0.258385	0.0229097	-28.2463	12.7017

**Table 4.**

$$P_r = 200, F_1 = 0.1, F_2 = 0.4, H = 0.3, E_c = 5.$$

$R_*$	$ D_0 $	$ D_1 $	$\tan \alpha_0$	$\tan \alpha_1$
5	2.73881	0.265488	-61.0054	5.35171
10	0.649884	0.0575502	-25.151	14.5618
15	0.29009	0.0244279	-29.1139	33.4444

**Table 5.**

$$P_r = 200, F_1 = 0.1, F_2 = 0.5, H = 0.2, R_* = 5.$$

$E_c$	$ D_0 $	$ D_1 $	$\tan \alpha_0$	$\tan \alpha_1$
5	2.74875	0.266414	-84.1425	5.12845
10	5.49751	0.532828	-84.1425	5.12845
15	8.24626	0.799242	-84.1425	5.12845

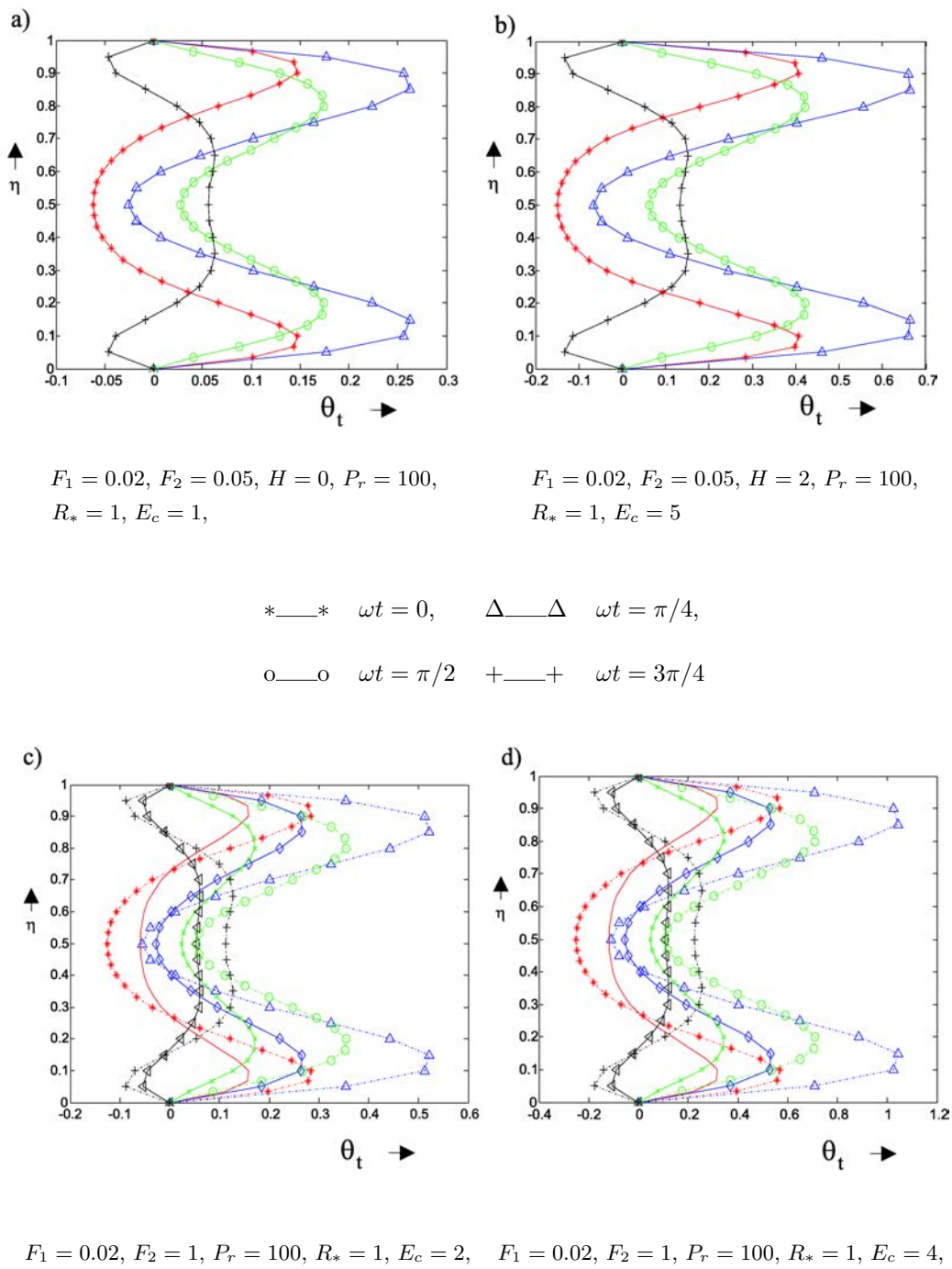
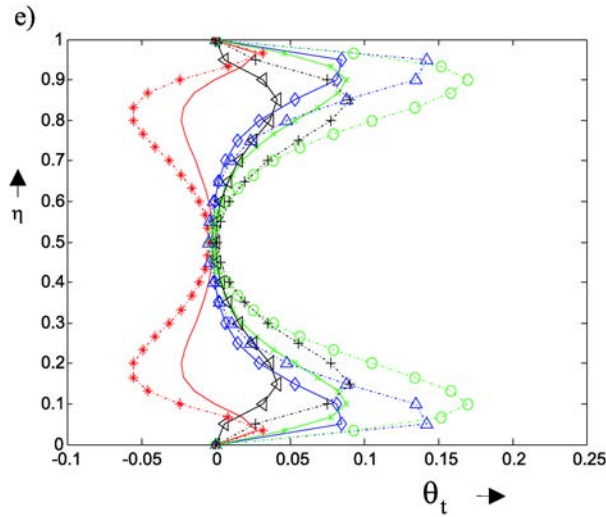


[FIG. 5]



$$F_1 = 0.02, F_2 = 1, Pr = 100, R_* = 2, Ec = 2$$

—	$H = 2$	$\omega t = 0,$	* - - *	$H = 0,$	$\omega t = 0,$
◇—◇	$H = 2$	$\omega t = \pi/4,$	△ - - △	$H = 0,$	$\omega t = \pi/4,$
×—×	$H = 2,$	$\omega t = \pi/2,$	o - - o	$H = 0,$	$\omega t = \pi/2,$
◁—▷	$H = 2,$	$\omega t = 3\pi/4,$	+ - - +	$H = 0,$	$\omega t = 3\pi/4.$

FIG. 5. Unsteady temperature profiles.

ACKNOWLEDGMENT

Authors acknowledge the financial support from D.R.D.O., India.

REFERENCES

1. A.S. BERMAN, *Laminar flow in channels with porous walls*, J. Appl. Phys., **24**, 1232–1235, 1953.
2. J.R. SELLARS, *Laminar flow in channels with porous walls at high suction Reynolds numbers*, J. Appl. Phys., **26**, 489–490, 1955.
3. S.W. YUAN, *Further investigation of laminar flow in channels with porous walls*, J. Appl. Phys., **27**, 267–269, 1956.
4. M. MORDUCHOW, *On laminar flow through a channel or tube with injection – application of method of averages*, Q.J. Appl. Math., **14**, 361–368, 1956.

5. A.S. BERMAN, *Laminar flow in an annulus with porous walls*, J. Appl. Phys., **29**, 71–75, 1958.
6. J.G. OLDROYD, *Non-Newtonian effects in steady motion of some idealized elastico-viscous liquids*, Proc. Roy. Soc. Lond., **A245**, 278–297, 1958.
7. Y.C. WANG, *Pulsatile flow in a porous channel*, J. Appl. Mech., **38**, 553–555, 1971.
8. S.A. VICTOR and V.L. SHAH, *Heat transfer to blood flowing in a tube*, Biorheology, **12**, 361–368, 1975.
9. G. RADHAKRISHNAMACHARYA and M.K. MAITI, *Heat transfer to pulsatile flow in a porous channel*, Int. J. Heat Mass Transfer, **20**, 171–173, 1977.
10. A.S. MUZUMDAR, *Advances in transport process*, Vol. 1, Wiley Eastern Ltd., 1980.
11. A.K. GHOSH and L. DEBNATH, *On heat transfer to pulsatile flow of a viscoelastic fluid*, Acta Mechanica, **93**, 169–177, 1992.
12. N. DATTA and D.C. DALAL, *Pulsatile flow and heat transfer of a dusty fluid through an infinitely long annular pipe*, Int. J. Multiphase flow, **21**, 515–528, 1995.
13. ALI J. CHAMKA, *Solutions for fluid-particle flow and heat transfer in a porous channel*, Int. J. Engg. Science, **34**, 1432–1439, 1996.
14. ZHIXIONG GUO, SEO YOUNG KIM and HYUNG JIN SUNG, *Pulsating flow and heat transfer in a pipe partially filled with porous medium*, Int. J. Heat Mass Transfer, **40**, 4209–4218, 1997.
15. T. MOSCHANDREOU and M. ZAMIR, *Heat transfer in a tube with pulsating flow and constant heat flux*, Int. J. Heat Mass Transfer, **40**, 2461–2466, 1997.
16. DAE-YOUNG LEE, SANG JIN PART and SUNG TACK RO, *Heat transfer in thermally developing region of a laminar oscillating pipe flow*, Cryogenics, **38**, 584–594, 1998.
17. A. OGULU and T.M. ABBEY, *Simulation of heat transfer on an oscillatory blood flow in an indented porous artery*, International communication in Heat and Mass Transfer, In press 2005.

*Received October 29, 2005.*

---